ORIGINAL ARTICLE

Cavitation in thin films of amorphous polymers from the static melt induced by thermal treatment

Masato Hashimoto[1] · Susumu Fujiwara[1] · Nan Lin[1] · Atsushi Doi[1] · Nozomi Katayama[1] · Junki Ootani[1] ·
Tomoko Mizuguchi[1]

Abstract

We discover a new cavitation phenomenon in amorphous polymers sandwiched between two thick slide glasses from the static melt induced by thermal treatment. By quenching atactic polystyrene (aPS) samples from the static melt under the glass transition temperature (T_g) and annealing them above T_g for thick slide glasses, cavities are created to relax the negative pressure. Cavity growth undergoes an Ostwald ripening-like process in cases of large molecular weight, while it undergoes a viscous fingering process in cases of small molecular weight. The induction time for cavity formation is found to decrease with the increase of the annealing temperature and with the decrease of molecular weight. In contrast, no cavities are observed in an aPS sample between two thin cover glasses because the negative pressure can be relaxed by bending the whole thin cover glasses.

Introduction

Cavitation, which is a term originally used in fluid mechanics, is the phenomenon by which vapor cavities are formed as a result of the negative pressure in a liquid [1, 2]. A cavity is a small liquid-free zone, such as a bubble or void. Cavitation is usually observed under the flow of low-molecular weight materials [1]. In polymeric materials, on the other hand, cavitation can be observed during the tensile deformation of crystalline polymers [3–7] and soft adhesives [8–12]. Yamaguchi, Doi, and co-workers proposed a simple theoretical model to describe the viscoelasticity and cavitation in soft adhesives [10–12].

Cavitation is also observed in the static melt during the crystallization of polymers induced by thermal treatment [13–19]. In isotactic polypropylene (iPP), Piorkowska et al. investigated the cavities induced when spherulites were grown between two cover glasses [16, 17]. They confirmed that a closed amorphous region of the polymers

exists between the two cover glasses and spherulites and concluded that cavitation results from the negative pressure that occurs in the closed amorphous region of the polymers due to the difference in density between the melt and the crystal. It was reported by Okui et al. that spherulites grow from the cavity, which is regarded as the nucleus, in poly(ethylene succinate) [18]. Furthermore, Galeski et al. confirmed that an ultrasonic wave is observed when the cavities created during crystallization in iPP are extinguished [13].

As mentioned above, the negative pressure generated during crystallization causes cavities in the polymer static melt. Then, is the crystallization process the only way to generate negative pressure in the polymer static melt? It is tacitly understood that thin cover glasses are not deformed by the negative pressure that occurs in the closed amorphous region of polymers during crystallization. Herein, we focus on the possibility that by quenching the amorphous polymer, the thick slide glasses may not be deformed, which would cause negative pressure, whereas thin cover glasses may be deformed.

In this study, we treated amorphous polymers to study the cavitation process in the static melt in a more direct way because cavitation is generated in the amorphous region. Especially, we investigated the cavitation process of atactic polystyrene (aPS), which is a typical amorphous general-purpose polymer. We observed whether cavities are created

✉ Masato Hashimoto
  hashima@kit.ac.jp

[1] Department of Macromolecular Science and Engineering,
  Graduate School of Science and Technology, Kyoto Institute of
  Technology Matsugasaki, Sakyo-ku, Kyoto 606-8585, Japan

in aPS samples using an optical microscope and examine the dependence of the cavitation process on the substrate and sample thicknesses, the molecular weight of the samples, and the annealing temperatures. We also discussed the relationship between the induction time for cavity creation and the annealing temperature.

Experimental procedure

The sample we used was aPS ($M_{\mathrm{w}} = 4.5 \times 10^4$, 2.6×10^5, and 2.3×10^6), which was purchased from Scientific Polymer Product Inc. (New York, USA). The aPS pellets were sandwiched between two thick slide glasses, which were 1300μm thick or two thin cover glasses, which were 150μm thick. We prepared samples with various values of thickness ranging from ca. 10 to 200 μm, using an aluminum foil spacer. Their linear dimensions were typically approximately 1.5 cm in diameter. The samples were subjected to heat treatment using the heater of a cooling and heating device (THM600; Linkam Scientific Instruments, Surrey, UK). The typical thermal histories used in this experiment are depicted in Fig. 1. The samples were melted at 260 °C for 10 min, quenched to room temperature, and annealed at 180 °C. The glass transition temperatures of the aPS samples with $M_{\mathrm{w}} = 4.5 \times 10^4$, 2.6×10^5, and 2.3×10^6, which were measured by DSC (5200 differential scanning calorimeter SSC thermal analysis system; Seiko Instruments, Chiba, Japan), were 90, 100, and 100 °C, respectively. The samples were observed in situ using an optical microscope with a hot stage. Micrographs were taken using a digital camera (COOLPIX 4500; Nikon Corp., Tokyo, Japan) and their video data were recorded by an HD video recording device (DMR-EH73V; Panasonic Corp., Osaka, Japan) via the video output of the digital camera attached to an optical microscope (ECLIPSE-ME600; Nikon Corp., Tokyo, Japan).

Results

We used two kinds of substrates, thin cover glasses and thick slide glasses, to investigate the dependence of the cavitation process on substrate and sample thickness. The thermal history shown in Fig. 1 was provided for an aPS sample. In the case of thin cover glasses, no cavities were observed, even after several hours of annealing. In the case of thick slide glasses, on the other hand, cavities were observed to generate. It should be noted that no cavities could be observed unless the sample was quenched under the glass transition temperature. Figure 2 shows an optical micrograph of a sample with a $M_{\mathrm{w}} = 2.6 \times 10^5$, which was 30μm thick, at an annealing time of ca. 10 s. This figure
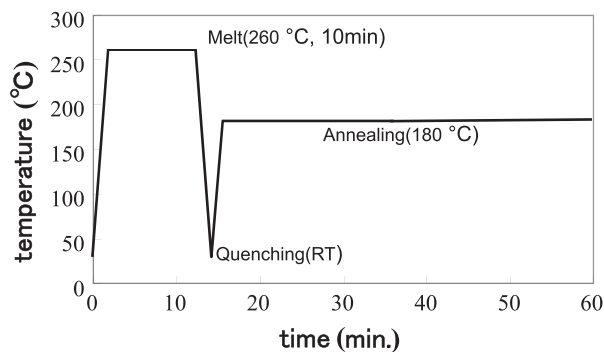

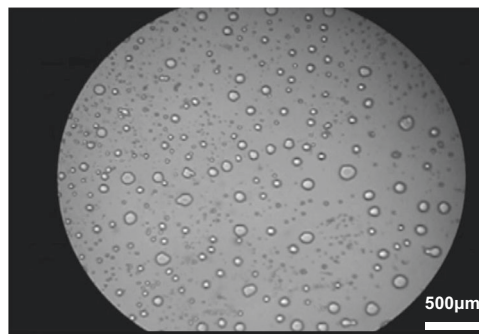**Fig. 1** Diagram of the typical thermal history used in this experiment

Fig. 2 Optical micrograph of cavities formed in an aPS sample ($M_{\mathrm{w}} = 2.6 \times 10^5$) at an annealing time of ca. 10 s. aPS, atactic polystyrene

tells us that various sizes of round cavities were observed rather homogeneously. It is worth noting that cavities were formed only at the central region of the specimen at the outset. It was experimentally confirmed that cavities could be formed only when the sample thickness was less than 100μm.

The formation and extinction processes of the cavities depend on the molecular weights of the samples. For an aPS sample with relatively large molecular weight ($M_{\mathrm{w}} = 2.6 \times 10^5$), typical examples of the cavity formation/extinction processes are shown in Fig. 3. Note that the heat treatment depicted in Fig. 1 was applied for the aPS sample. As shown in Fig. 3a, few cavities were observed for an annealing time of ca. 8 s, which indicates the existence of an induction time for the formation of cavities. Let me here note that there may exist much smaller cavities, which cannot be identified at the resolution of the applied optical microscope (ca. 0.2μm). After the induction time elapsed, cavities were observed to grow in various places (Fig. 3b–d). During the cavity-creation process, the number of cavities was found to increase. The size of the cavities formed at an annealing time of ca. 12 s ranged from several micrometers to several tens of micrometers in diameter (Fig. 3d). It can also be found from Fig. 3d, e that the relatively small cavities indicated by gray dots, whose sizes

Fig. 3 Optical micrographs of an aPS sample ($M_w = 2.6 \times 10^5$) at various annealing times: **a**) 8.2 s, **b**) 8.4 s, **c**) 8.6 s, **d**) 12 s, **e**) 20 s, **f**) 2 min, **g**) 15 min, and **h**) 65 min. The thermal history shown in Fig. 1 was provided for the aPS sample. aPS, atactic polystyrene
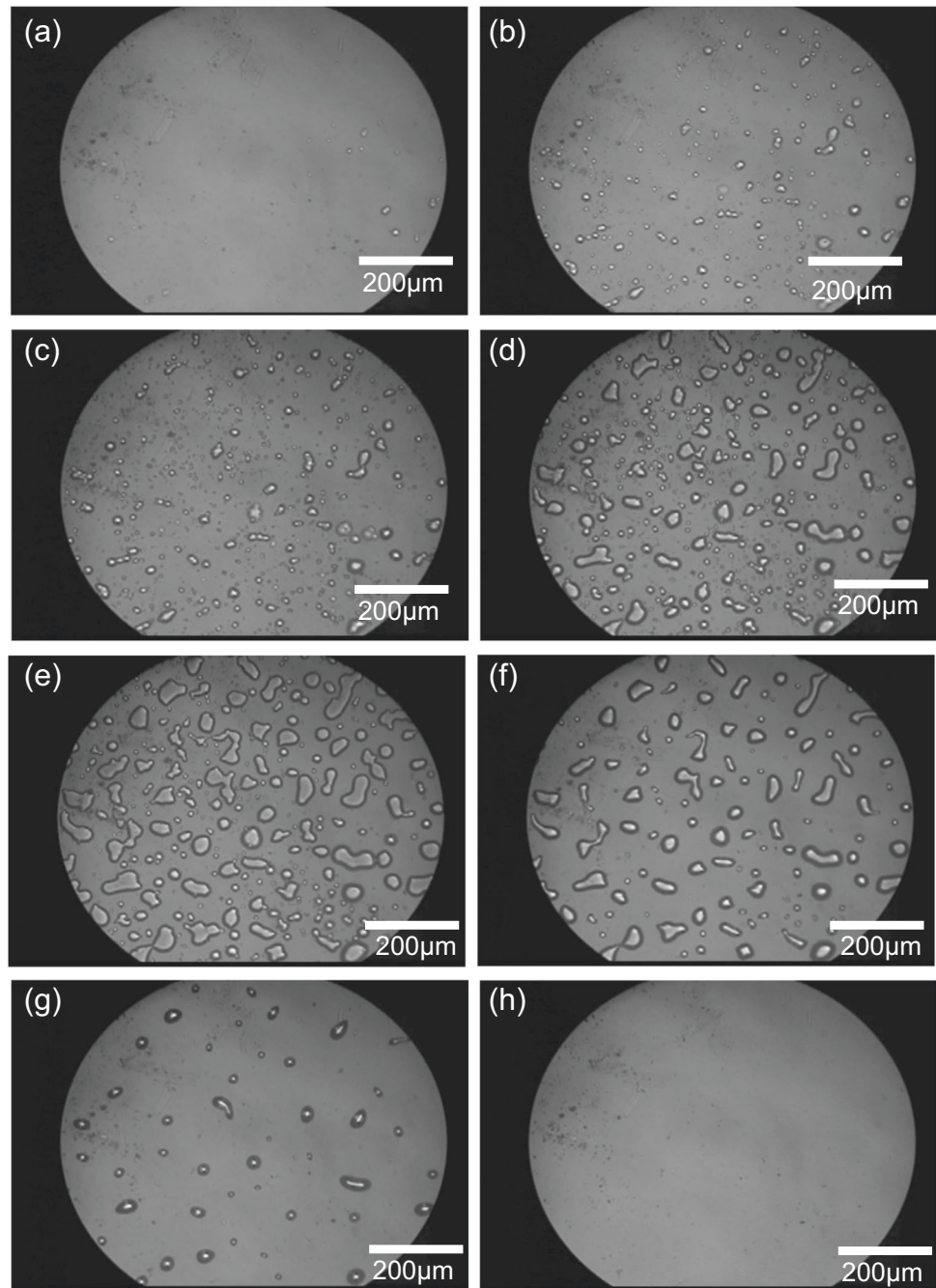
were smaller than 1 μm in diameter, were observed at the annealing time of 12 s and disappeared at that of 20 s. The relatively large cavities, on the other hand, were found to grow until an annealing time of ca. 20 s. After ceasing growth, all the cavities started to contract and eventually disappeared completely (Fig. 3f–h). This finding shows that in the present case, the cavity growth underwent an Ostwald ripening-like process. The same kind of cavity formation/extinction process was also observed at the annealing temperatures of 170 and 160 °C, except that the cavity-induction, -formation, and -extinction times became longer

than those at the annealing temperature of 180 °C. It should be noted that in some cases, not all the cavities disappeared, and cavities with finite sizes remained.

Image processing was performed for the sample with a $M_w = 2.6 \times 10^5$ to investigate the above-mentioned cavity formation/extinction process quantitatively. First, the outlines of the cavities were extracted, and then the average radius of the cavities was calculated. We regarded Fig. 3h as the background, and the vaue was subtracted from that of each image in Fig. 3. Figure 4 shows the temporal evolution of the average radius as a log–log plot. It is noteworthy that
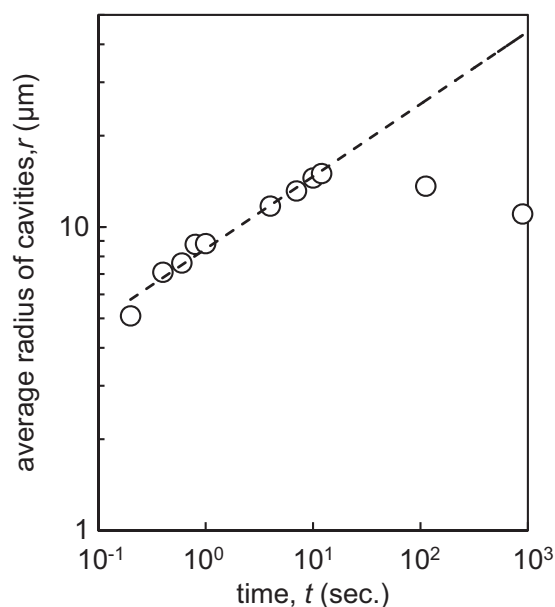
Fig. 4 Time dependence of the average cavity radius for an aPS sample with a $M_w = 2.6 \times 10^5$. The broken line represents a power function with an exponent of 0.213. aPS, atactic polystyrene

we ignored the outlines with sizes of 1 or 2 dots since small outlines can be regarded as dust and dirt. We should also note that the time of the abscissa is the annealing time minus the induction time (8 s). Figure 4 tells us that the average radius of the cavities increased according to a power law with an exponent of 0.213 and began to decrease at approximately 10 s.

For an aPS sample with a relatively small molecular weight ($M_w = 4.5 \times 10^4$), on the other hand, different formation/extinction processes of the cavities were observed, as shown in Fig. 5. The heat treatment depicted in Fig. 1 was also applied in this case. As shown in Fig. 5a, few cavities were observed for an annealing time of ca. 9 s, which indicates that an induction time for cavity formation exists in this case also. After the induction time elapsed, round cavities started to grow (Fig. 5b) and, branched off (Fig. 5c), and fingering cavity growth was then observed (Fig. 5d). This result indicates that the present cavity growth underwent a viscous fingering process. After ceasing growth, the grown edges became rounded and the contour lines of the cavities blurred (Fig. 5e). Afterward, all the cavities started to contract and eventually disappeared completely (Fig. 5f–h). There was little variation in the number of cavities during the cavity formation/extinction processes (Fig. 5b–h) unlike the case with a relatively large molecular weight. As with the case of a relatively large molecular weight, there were some cases wherein not all the cavities disappeared and cavities with finite sizes remained. It is worth noting that, in some cases, cavities with a dendritic shape were observed.

As mentioned above, the induction time for the formation of cavities depends on the annealing temperatures. Figure 6 shows the annealing-temperature dependence of the induction time for aPS samples with various molecular weights. The same thermal history as shown in Fig. 1 was provided for the aPS samples, except for the annealing temperature. It was found that the cavity-formation process for the aPS samples with $M_w = 2.6 \times 10^5$ and 2.3×10^6 is Ostwald ripening-like while that for the aPS sample with a $M_w = 4.5 \times 10^4$ is viscous fingering, irrespective of the annealing temperatures.

Discussion

As stated in the previous section, cavities were observed by quenching an aPS melt under the glass transition temperature in the case of the thick slide glasses while no cavities were observed in the sample between the thin cover glasses. We here discuss the reason why cavitation occurred in the former case. Let us consider the situation in which the thermal history shown in Fig. 7(I) is provided for the aPS sample sandwiched by the slide glasses. The aPS sample at room temperature (RT), which is lower than the glass transition temperature T_g, expands laterally after heating the sample to T_1 ($> T_g$) (Fig. 7(II) a, b). After quenching the sample again to RT ($< T_g$), its size remains almost unchanged since it is in a frozen state (Fig. 7(II) c). After rapid heating of the sample to T_2, which is above T_g but below T_1, the molecules become locally mobile (because $T_2 > T_g$) and the whole sample tends to shrink (because $T_2 < T_1$), but the time scale of the volume change of the whole sample is much larger than that of the local molecular motion, which leads to the occurrence of a negative pressure (Fig. 7(II) d). After a further annealing of the sample at T_2, which is above T_g, cavities are generated to relax the negative pressure (Fig. 7(II) e). Let us roughly estimate the magnitude of the negative pressure generated in Fig. 7(II) d. The sample is considered to be a homogeneous solid. When expanding the sample from Fig. 7(II) a to Fig. 7(II) b, the volume becomes $V_{RT} (1 + \beta(T_1\text{-RT}))$, where RT is the room temperature, V_{RT} is the volume at RT in Fig. 7(II) a, and β is the thermal expansion of polystyrene. The volumes in Fig. 7(II) b–d are all assumed to be the same. The volume at T_2 should be $V_{RT} (1 + \beta(T_2\text{-RT}))$, when the system is in equilibrium. Therefore, the volume increment from equilibrium is $V_{RT} \beta(T_1\text{-}T_2)$. Negative pressure is generated by this strain: $\beta(T_1\text{-}T_2)$. The negative pressure, P, can be estimated by $P = \alpha\beta(T_1\text{-}T_2)$, where α is the bulk modus. Since $\alpha \approx 4$ GPa, $\beta \approx 5 \times 10^{-4} \, K^{-1}$ [20], $T_1 = 260 \, °C$, and $T_2 = 180 \, °C$, P is calculated as 160 MPa.

Concerning the spacial distribution of the cavities, our experimental results show that the cavities tend to be

Fig. 5 Optical micrographs of an aPS sample ($M_w = 4.5 \times 10^4$) at various annealing times: **a**) 9.5 s, **b**) 12 s, **c**)15 s, **d**) 17 s, **e**) 22 s, **f**) 35 s, **g**) 40 s, and **h**) 3 min 50 s. The thermal history shown in Fig. 1 was provided for the aPS sample. aPS, atactic polystyrene
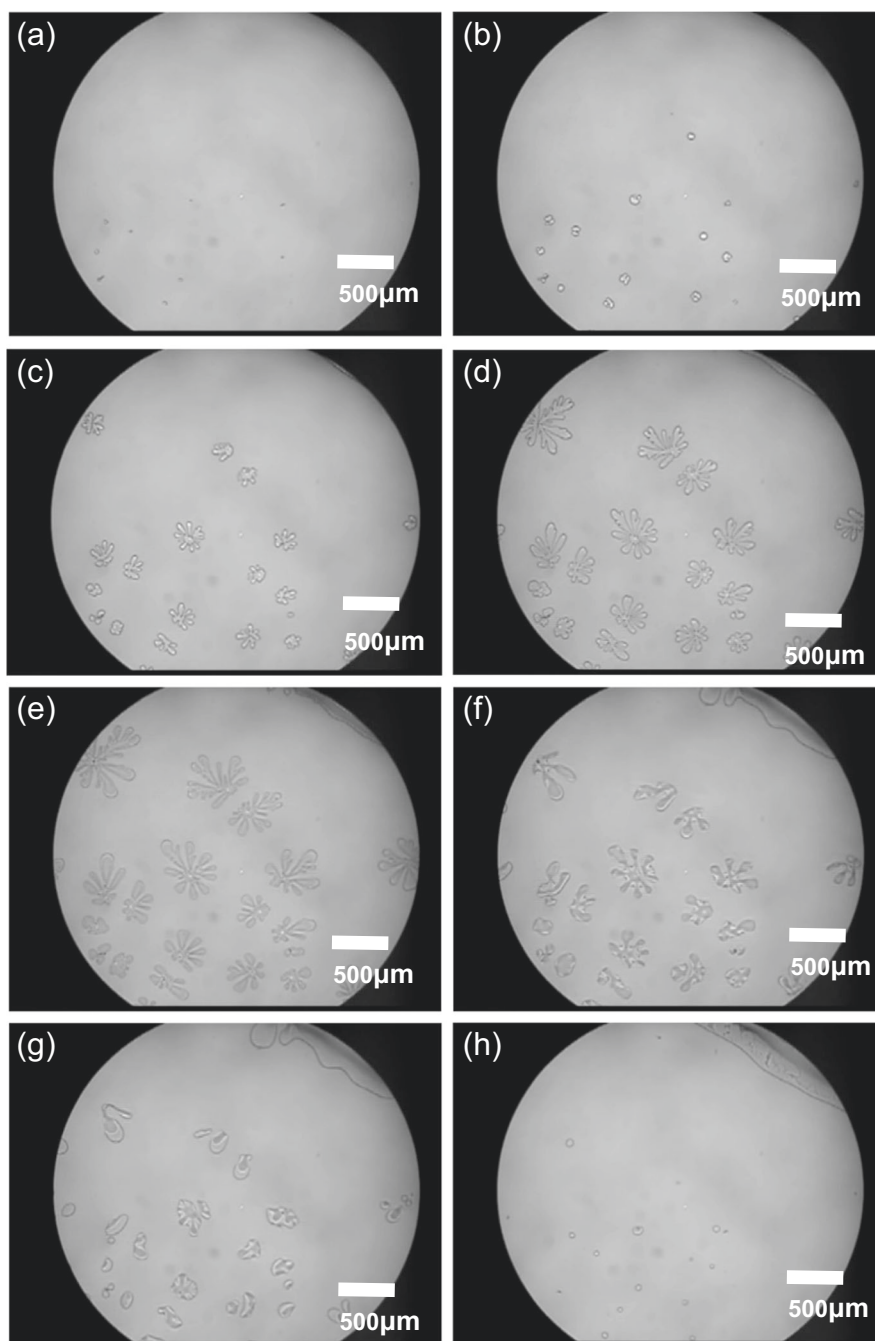
generated in the middle part of the sample along the horizontal direction. Considering these experimental findings, it seems reasonable to conclude that the degree of negative pressure in the middle part of the sample is larger than that in the outer parts of the sample along the horizontal direction. In the case of thin cover glasses, such negative pressures can be relaxed by bending the whole cover glasses (Fig. 8a). In the case of thick slide glasses, on the other hand, cavities are generated to relax the negative pressure because the slide glasses are too thick to bend (Fig. 8b). As

far as we know, no cavities have so far been observed from static melts in the case of amorphous polymers. The reason for this is that most experiments use thin cover glasses instead of thick slide glasses. Incidentally, the cavity-formation process during crystallization is also shown in Fig. 8c according to refs. [16, 17] for the case of an iPP melt sandwiched by thin cover glasses. As shown in the middle part of Fig. 8c, there exist several closed amorphous regions of polymers (white regions), which are surrounded by two cover glasses and spherulites after crystallization. The
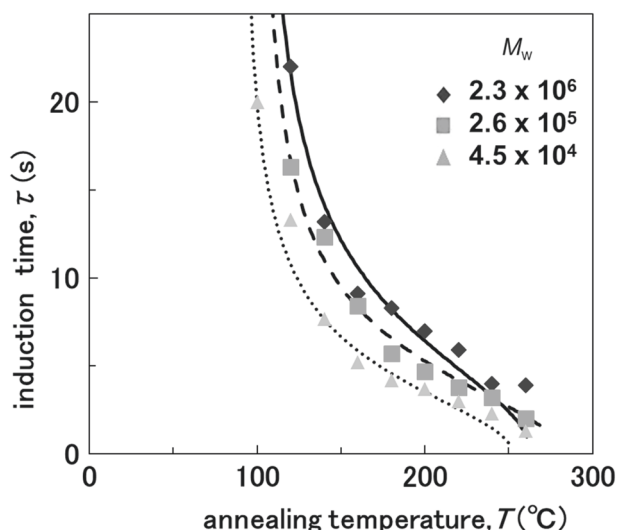
Fig. 6 Annealing-temperature dependence of the induction time for aPS samples with various molecular weights ($M_w = 4.5 \times 10^4$, 2.6×10^5, and 2.3×10^6). The solid, broken, and dotted curves are the fitting curves produced by equation (1). aPS, atactic polystyrene

negative pressure occurs in the closed amorphous regions of the polymers due to the difference in the density between the melt and the crystal. Afterward, the sample is relaxed by cavity formation in the closed amorphous regions (right part of Fig. 8c).

It is worth mentioning that cavities could be observed in other amorphous polymers such as poly(vinyl chloride), polycarbonate, and poly(methyl methacrylate) by a similar thermal treatment to that shown in Fig. 7(I) (Fig. 9).

As revealed in the previous section, the cavity growth underwent an Ostwald ripening-like process in the case of relatively large molecular weights (i.e., relatively high viscosity), while it underwent a viscous fingering process in the case of relatively small molecular weights (i.e., relatively low viscosity). The latter result indicates that a cavity branches off and grows, rather than a new cavity being generated in the case of relatively low viscosity because there is little variation in the number of cavities in the case of relatively small molecular weights or relatively low viscosity (Fig. 5f–h). This result indicates that it takes a

Fig. 7 I) Diagram of the thermal history provided for the aPS sample. **II**) Schematic illustration of the formation mechanism of cavities in the case of thick slide glasses. **a–e** Correspond to the filled circles in (**I**). The thick arrows in (**II**)**d** indicate negative pressures in the sample. Note that the dimension of the sample along the perpendicular direction is magnified by approximately 10^4 times. aPS, atactic polystyrene
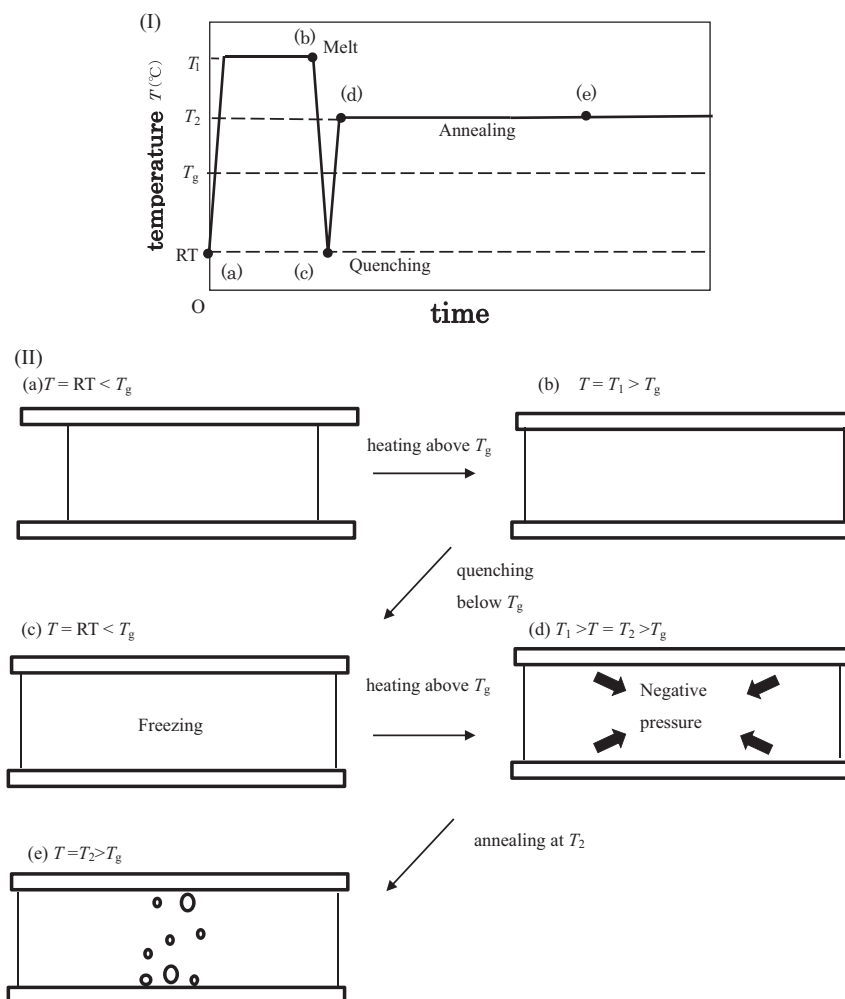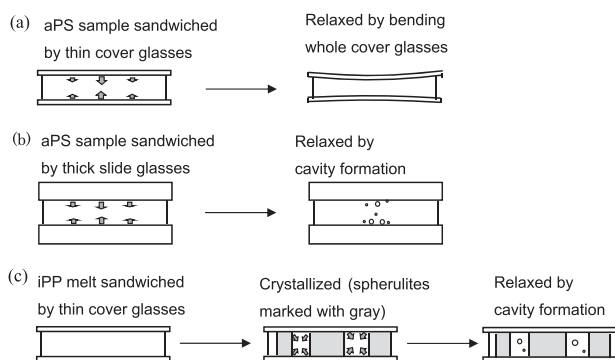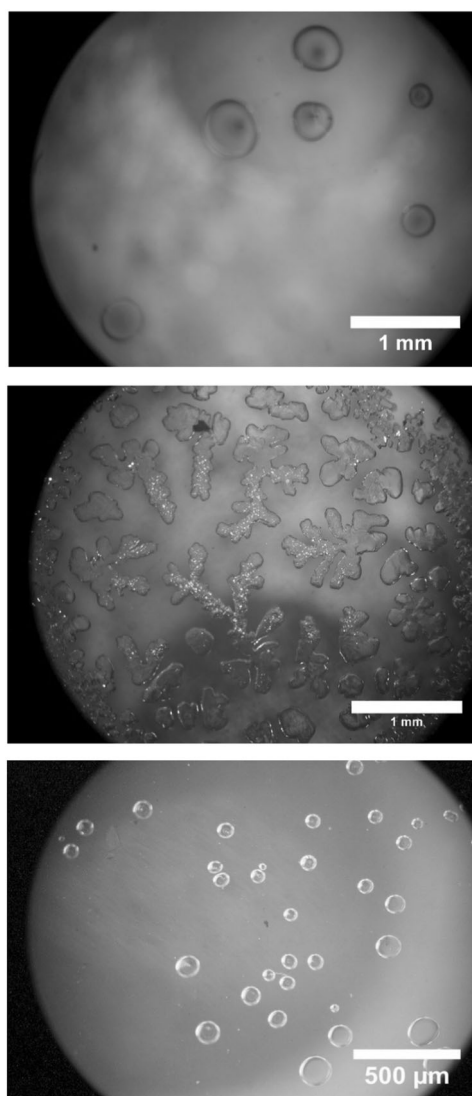
Fig. 8 Schematic illustration of the relaxation processes of negative pressure in the case of **a**) an aPS sample sandwiched by thin cover glasses, **b**) an aPS sample sandwiched by thick slide glasses, and **c**) an iPP melt sandwiched by thin cover glasses. The thick arrows in (**a**) and (**b**) indicate the negative pressures at the interfaces between the sample and the thin cover or thick side glasses. White and gray regions in (**c**) represent amorphous and crystal regions, respectively. Note that the dimension of a sample along the perpendicular direction is magnified by approximately 10^4 times. aPS, atactic polystyrene; iPP, isotactic polypropylene

Fig. 9 **a**) Optical micrograph of a polycarbonate sample after melting at 290 °C for 15 min, quenching to approximately 0 °C, and annealing at 180 °C for some time. **b**) Optical micrograph of a polyvinyl chloride sample after melting at 190 °C for 40 min, quenching to approximately 0 °C, and annealing at 190 °C for some time. **c**) Optical micrograph of a poly(methyl methacrylate) sample after melting at 260 °C for 15 min, quenching to room temperature, and annealing at 170 °C for 5 min

long time to form a new cavity compared to the time scale of cavity formation/extinction. The viscous fingering phenomenon is probably due to Saffman–Taylor instabilities [21], but it is hard to answer why the fingering patterns are generated in low-molecular weight polymers. Fingering and cavitation phenomena are also observed in traction experiments on viscous liquids highly confined between parallel plates by Poivet et al. [22, 23]. These studies concluded that fingering is favored for low traction velocities, low confinement, and low viscosity, whereas cavitation or the nucleation of bubbles occurs under the opposite conditions.

Concerning the temporal evolution of the average radius of the cavities, it is well known that the exponent of the power law for common Ostwald ripening is 1/3 [24]. Our calculated exponent for the cavitation is 0.213, which is smaller than 1/3 (Fig. 4). This discrepancy suggests that the overall shrinkage had already occurred before 10 s.

Here, let us consider the relationship between the induction time (τ) and the annealing temperature (T_2) shown in Fig. 6. At all molecular weights, the induction time seems to become infinite at around the glass transition temperature. It is also found that the induction time decreases with the increase of annealing temperature and approaches zero. The larger the molecular weight, the longer is the induction time at each annealing temperature. Surprisingly, the induction time is increased only slightly despite the molecular weight changes of approximately 3 orders of magnitude. The annealing-temperature dependence of the induction time for cavity formation is almost independent of the formation and extinction processes, the Ostwald ripening-like process, or the viscous fingering process because the induction time for cavity formation is determined before the cavities are

formed. To further obtain the quantitative relationship between the induction time and annealing temperature, we show, in Fig. 10, a plot of the square of the induction time (τ^2) vs the reciprocal of the temperature minus the glass transition temperature ($1/(T_2-T_g)$). We use $1/(T_2-T_g)$ as an abscissa because τ is divergent around T_g. Figure 10 indicates that the data points are well fitted by

$$\tau^2 = A\left(\frac{1}{T_2 - T_g} - \varepsilon\right), \tag{1}$$

where A and ε are positive constants. The values of A and ε are $A = 1.1 \times 10^4$, 6.2×10^3, and 4.3×10^3, and $\varepsilon = 6.1 \times 10^{-3}$,
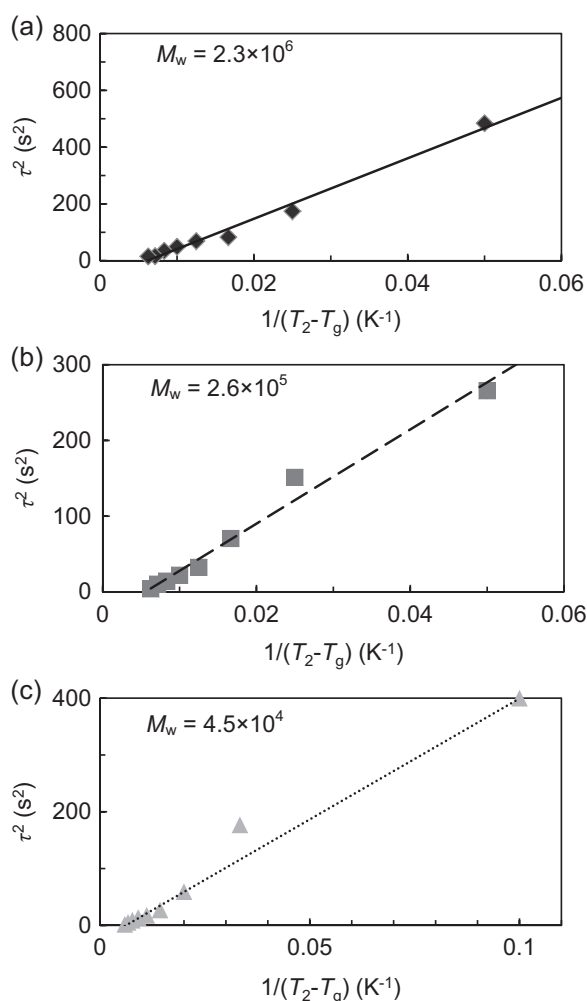
Fig. 10 $1/(T_2-T_g)$ dependence of τ^2 for various molecular weights: **a)** $M_w = 2.3 \times 10^6$, **b)** 2.6×10^5, and **c)** 4.5×10^4. The solid, broken, and dotted lines are the least-squares lines

5.5×10^{-3}, and 6.2×10^{-3} for samples with molecular weights 2.3×10^6, 2.6×10^5, and 4.5×10^4, respectively. According to the schematic illustration of cavity formation (Fig. 7), τ should be zero when T_2 equals $T_1(= 260\,°C)$. However, it is found from Fig. 6 that τ has a finite value at $T_2(= 260\,°C)$, which clearly shows the occurrence of cavitation at T_2, because the system is not in equilibrium and local strain exists just after heating the sample to T_2 $(= T_1)$.

Finally, we comment on the cover glasses and slide glasses. Cover glasses and slide glasses differ not only in thickness but also in materials. In our experiments, cover glasses made from borosilicate glasses and slide glasses made from soda-lime-silica glasses were used. As mentioned above, cavitation occurred in the case of thick slide glasses whereas no cavities were observed in the case of thin cover glasses. To confirm whether the substrate thickness determines the occurrence of cavitation, we used thick

glasses made from borosilicate glass (TEMPAX Float®), whose thickness was almost the same as that of the thick slide glasses. As a result, we observed cavities when the thermal history shown in Fig. 1 was provided for an aPS sample. It is, therefore, ascertained that substrate thickness is a determining factor in the occurrence of cavitation.

Conclusions

We investigated the cavitation processes of aPS samples sandwiched between two thin cover glasses or thick slide glasses from static melt by thermal treatment using an optical microscope. Cavities were observed by quenching an aPS sample from the static melt under T_g and annealing it above T_g for the thick slide glasses, whereas no cavities were observed in the sample between the thin cover glasses. This is the first time that cavitation phenomena were observed in amorphous polymers from the static melt without processing. We also ascertained that cavities could be formed in other amorphous polymers such as poly(vinyl chloride), polycarbonate, etc. The degree of negative pressure in the middle part of the sample was found to be larger than that in the outer parts of the sample along the horizontal direction. For thin cover glasses, such negative pressures can be relaxed by bending the whole cover glasses.

The cavity growth underwent an Ostwald ripening-like process in the case of high viscosity (large M_w), while it underwent a viscous fingering process in the case of low viscosity (small M_w). The average radius of the cavities was found to increase according to a power law during cavity growth in the case of high viscosity.

The induction time, τ, was found to decrease with the increase of annealing temperature, T_2. The induction time was only slightly increased with molecular weight, despite a molecular weight change of approximately 3 order of magnitude. The annealing-temperature dependence of the induction time for cavity formation is almost independent of the formation and extinction processes, the Ostwald ripening-like process, or the viscous fingering process, and τ^2 is linearly related to $1/(T_2-T_g)$ because the induction time for cavity formation is determined before the cavities are formed.

Compliance with ethical standards

References

1. Knapp RT, Daily JW, Hammitt FG. Cavitation, engineering societies monographs. New York: McGRAW-HILL Co; 1970.
2. Brenen CE. Cavitation and bubble dynamics. New York: Oxford University Press; 1995.
3. Pawlak A, Galeski A. Plastic deformation of crystalline polymers: the role of cavitation and crystal plasticity. Macromolecules. 2005;38:9699–9697.
4. Pawlak A, Galeski A. Cavitation during tensile deformation of polypropylene. Macromolecules. 2008;41:2839–51.
5. Galeski A, Rozanski A. Cavitation during drawing of crystalline polymers. Macromol Symp. 2010;298:1–9.
6. Castagneta S, Girault S, Gacougnollea JL, Dang P. Cavitation in strained polyvinylidene fluoride: mechanical and X-ray experimental studies. Polymer (Guildf). 2000;41:7523–30.
7. Pawlak A. Cavitation during tensile deformation of high-density polyethylene. Polymer (Guildf). 2007;48:1397–409.
8. Chiche A, Dollhofer J, Creton C. Cavity growth in soft adhesives. Eur Phys J E. 2005;17:389–401.
9. Chikina I, Gay C. Cavitation in adhesives. Phys Rev Lett. 2000;85:4546–9.
10. Yamaguchi T, Morita H, Doi M. Modeling on debonding dynamics of pressure-sensitive adhesives. Eur Phys J E. 2006;20:7–17.
11. Doi M, Yamaguchi T. Analytical solution for the deformation of pressure sensitive adhesives confined between two rigid plates. J Nonnewton Fluid Mech. 2007;145:52–56.
12. Yamaguchi T, Creton C, Doi M. Simple model on debonding of soft adhesives. Soft Matter. 2018;14:6206–13.
13. Galeski A, Koenczoel L, Piorkowska E, Baer E. Acoustic emission during polymer crystallization. Nature. 1987;325:40–41.
14. Monasse B, Haudin JM. Effect of random copolymerization on growth transition and morphology change in polypropylene. Colloid Polym Sci. 1988;266:679–87.
15. Thoman R, Wang Ch, Kressler J, Mulhaupt R. Negative pressure effects during the isothermal crystallization of isotactic poly(propylene) studied by light and atomic force microscopy. Macromol Chem Phys. 1996;197:1085–91.
16. Nowacki R, Kolasinska J, Piorkowska E. Cavitation during isothermal crystallization of isotactic polypropylene. J Appl Polym Sci. 2001;79:2439–48.
17. Nowacki R, Piorkowska E. Influence of solid particles on cavitation in poly(methylene oxide) during crystallization. J Appl Polym Sci. 2007;105:1053–62.
18. Imanishi Y, Nakamura K, Takita T, Umemoto S, Okui N. Characterizations for negative pressures during spherulite growth and cavitation phenomena [I]. Polym Prep Jpn. 2006;55:805.
19. Pawlak A, Piorkowska E. Effect of negative pressure on melting behavior of spherulites in thin films of several crystalline polymers. J Appl Polym Sci. 1999;74:1380–5.
20. Brandrup J, Immergut EH. Polymer handbook. 3rd ed. New York: John Wiley & Sons; 1989.
21. Saffman PG, Taylor GI. The penetration of a fluid into a porous medium or Hele-Shaw cell containing a more viscous liquid. Proc Roy Soc London Ser A. 1958;A245:312–29.
22. Poivet S, Nallet F, Gay C, Fabre P. Cavitation-induced force transition in confined viscous liquids under traction. Europhys Lett. 2003;62:244–50.
23. Poivet S, Nallet F, Gaya C, Teisseire J, Fabreb P. Force response of a viscous liquid in a probe-tack geometry: fingering versus cavitation. Eur Phys J E. 2004;15:97–116.
24. Voorhees PW. The theory of Ostwald ripening. J Stat Phys. 1995;38:231–52.